

BBABIO 43172

Thermodynamic properties of D1/D2/cytochrome *b*-559 reaction centres investigated by time-resolved fluorescence measurements

P.J. Booth¹, B. Crystall¹, L.B. Giorgi¹, J. Barber², D.R. Klug¹ and G. Porter¹

¹ Photochemistry Research Group, Department of Biology, and ² AFRC Photosynthesis Research Group, Department of Biochemistry, Imperial College, London (U.K.)

(Received 2 August 1989)

(Revised manuscript received 21 November 1989)

Key words: Photosystem II; Fluorescence spectroscopy; Reaction center; Time resolved spectroscopy; Electron transfer; Free energy

Photosystem II reaction centres have been studied using time-correlated single photon counting to provide time-resolved fluorescence information. Comparative quantum yield measurements suggest that up to 94% of the chlorophyll in these preparations is coupled to the charge-separation pathway. Analysis of time-resolved fluorescence data suggests a free-energy gap between the excited chlorophyll special pair and the primary radical pair of $\Delta G(\text{P680}^+ \text{Ph}^- - \text{P680}^*) = -0.11$ eV at 277 K. Measurements of this free-energy difference between 277 K and 77 K show that between 220 K and 77 K the contributions of entropy and enthalpy are $\Delta S(\text{P680}^+ \text{Ph}^- - \text{P680}^*) = +3.8 \cdot 10^{-4}$ eV · K⁻¹ and $\Delta H(\text{P680}^+ \text{Ph}^- - \text{P680}^*) = -5.0 \cdot 10^{-3}$ eV, respectively. Thus the charge transfer reaction is dominated by entropy contributions between 77 K and 220 K, the ratio of entropy to enthalpy at 220 K being 17:1. The relationship between ΔG and temperature is non-linear over the range 220–270 K, which indicates that enthalpy and/or entropy are temperature dependent in this region.

Introduction

The isolation [1,2] of the D1/D2/cytochrome *b*-559 complex that constitutes the Photosystem II reaction centre has provided an opportunity to study the kinetics of the charge-separated state without the complication caused by the presence of subsequent quinone acceptors. The stabilisation of this labile particle [3] has further facilitated spectroscopic studies.

The D1/D2 complex contains 4 chlorophyll-*a* molecules, 2 pheophytin-*a* molecules, 1 cytochrome *b*-559 and some β -carotene, but it contains no measurable quantities of plastoquinone [1,2].

Transient absorption spectroscopy of the D1/D2/cytochrome *b*-559 reaction centre complex has indicated the presence of a component decaying with a lifetime of 25–35 ns, assigned to the lifetime of the primary radical pair [4,5]. Time-resolved fluorescence studies [6,7] have

shown a lifetime of 25–35 ns which has been attributed to the recombination of the primary radical pair. However, the fluorescence from this component was observed to be less than 2% of the total light emitted. Further time-resolved fluorescence measurements of stabilised D1/D2 reaction centres at 277 K have shown a lifetime of 37 ns, contributing 44% of the total fluorescence, which has been assigned to the singlet excited state of P680 (P680*) in equilibrium with the primary radical pair, P680⁺Ph⁻ [3]. The remainder of the fluorescence is predominantly a 6.5 ns component attributed to chlorophyll which is energetically uncoupled from the process of charge separation.

P680* is formed when the D1/D2/cytochrome *b*-559 reaction centre complex absorbs light. It is oxidised in approx. 3 ps [8] and an electron transfer equilibrium between P680* and the primary radical pair, (P680* \rightleftharpoons P680⁺Ph⁻), is established. The singlet-state radical pair initially formed may then undergo singlet-triplet mixing to yield the triplet state of the radical pair. Charge recombination from the triplet radical pair gives rise to the P680 triplet state, which decays to the ground state in the absence of oxygen with a lifetime of 1 ms [9]. Charge recombination of the singlet radical-pair state, to form either P680 or P680*, competes with the recombination of the triplet radical pair. P680* can decay to

Abbreviations: Ph, pheophytin; SPC, single photon counting; fwhm, full width half maximum; DBMIB, 2,5-dibromo-3-methyl-6-isopropyl-*p*-benzoquinone; BPh, bacteriopheophytin; PS II, Photosystem II.

Correspondence address: P.J. Booth, Photochemistry Research Group, Department of Biology (East Wing), Imperial College, Prince Consort Road, London, SW7 2BB, U.K.

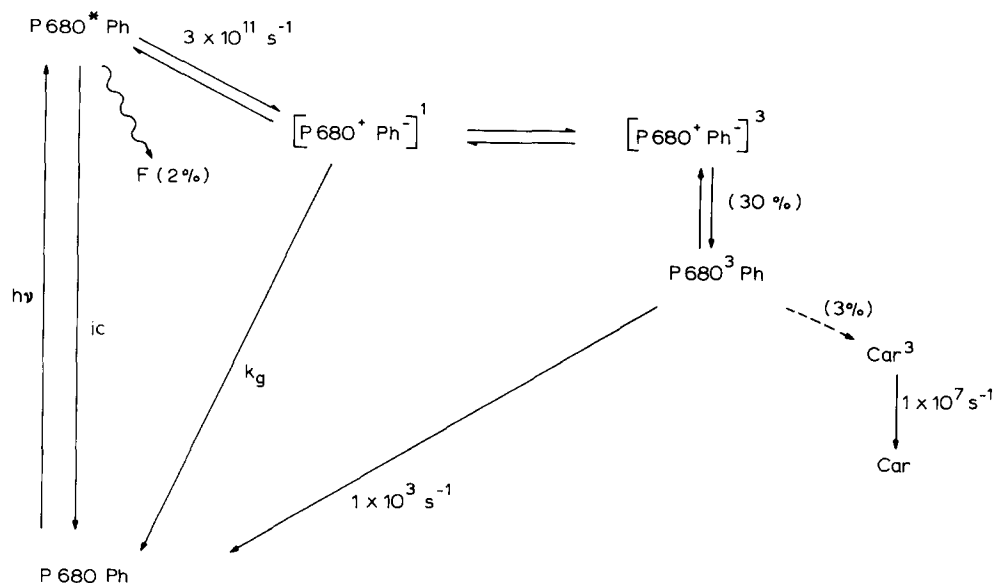


Fig. 1. Kinetic scheme in the D1/D2 reaction centre. Values in brackets give the percentage yield of the particular pathway. ic, internal conversion; k_g , rate of charge recombination of radical pair directly to the ground state; F , fluorescence; Car, β -carotene. The dashed line indicates a possible pathway for the formation of β -carotene triplet.

P680 by internal conversion or fluorescence. The dominant deactivation pathways, however, seem to be via triplet formation (the quantum yield of triplet formation is 0.3 [9]) and internal conversion. A possible kinetic scheme in the D1/D2 reaction centre is shown in Fig. 1.

The yield of the charge-recombination fluorescence and the position of the Q_y absorption peak have been found to be useful measures of the activity of the D1/D2 complex [3,6,10]. Reduction in the yield of the 37 ns lifetime correlates with a blue shift in the position of the Q_y absorption band. It is assumed that a high yield of charge-recombination fluorescence indicates a high yield of radical-pair formation. It has been established that removing oxygen from the sample significantly improves the stability of the D1/D2 preparation [3,11]. Reduced stability in the presence of oxygen is probably caused by oxygen quenching of the P680 triplet state, resulting in the formation of highly oxidising singlet oxygen [11,12].

In this paper, the free-energy difference between P680* and the radical pair is calculated from time-resolved fluorescence data. Results are presented over the temperature range 77 K to 277 K. These data provide information about the contributions of entropy and enthalpy to the free-energy difference between the reactants and products of the electron transfer reaction.

Materials and Methods

Sample preparation

Photosystem II reaction centre complexes were prepared from pea chloroplasts as described by Chapman et al. [13] with the following changes. Exchange to 2

mM dodecyl maltoside was carried out after the first column purification in Triton X-100 by elution from a DEAE-Fractogel ion-exchange column with a linear NaCl gradient of $5 \text{ mM} \cdot \text{ml}^{-1}$ in 50 mM Tris-HCl buffer containing 2 mM dodecyl maltoside at pH 7.2. A single protein peak was eluted and the samples were stored at 277 K. Samples were suspended in a buffer of 50 mM Tris-HCl (pH 8 at room temperature) containing 2 mM dodecyl maltoside to give a final chlorophyll concentration of $10 \mu\text{g} \cdot \text{ml}^{-1}$ (unless otherwise stated). Anaerobic conditions were achieved by adding 5 mM glucose, $0.1 \text{ mg} \cdot \text{ml}^{-1}$ glucose oxidase and $0.05 \text{ mg} \cdot \text{ml}^{-1}$ catalase to the sample in a sealed cuvette. Samples were allowed to stand for 10 min before each experiment to ensure maximum removal of oxygen. All experiments were performed on anaerobic samples at a temperature of 277 K, or below, unless otherwise stated.

Spectroscopy

Steady-state absorption and fluorescence measurements were made using a Perkin-Elmer 554 spectrophotometer and a Perkin-Elmer MPF-4 fluorimeter.

Fluorescence lifetimes were measured using time-correlated single photon counting (SPC) [14,15]. The apparatus consisted of a modelocked Coherent Antares YAG laser, synchronously pumping a cavity-dumped rhodamine 6G dye laser. This provided a 3.7 MHz train of 8 ps pulses. Emission wavelength was selected with a 0.3 m Hilger-Watts monochromator and detected using a red-sensitive Hamamatsu R1564.U01 microchannel plate photomultiplier tube. The instrument response function was measured to be 120 ps (fwhm) using a Ludox scattering solution. The SPC electronics consisted of two Ortec 584 constant-fraction discrimina-

tors, an Ortec 457 biased time to amplitude converter and a Tracor Northern EC1 multi-channel analyser with 512 channels. All samples were excited at 615 nm with an average power of 20 mW. Samples were also stirred in those experiments performed at 277 K.

Variable temperature measurements were made using an Oxford Instruments DN 1704 liquid nitrogen cryostat. This allowed the sample temperature to be regulated between 77 K and 277 K. Clear glasses were obtained by the addition of 80% glycerol to the buffer and cooling the samples slowly in the dark over a period of 1 or 2 h.

During data collection, the samples were subjected to approx. 5 min of laser excitation at an average power of 20 mW. This yielded between 10 000 and 20 000 counts peak channel. All samples showed a Q_y band absorption peak of (675.9 ± 0.2) nm before and after all time-resolved measurements, unless otherwise stated.

The incident light intensity was $6.2 \cdot 10^{16}$ photons \cdot s^{-1} , over 0.1 cm^3 of sample. The optical absorbance of the samples is approximately 0.15 at 615 nm and 30% of the quanta absorbed appear as P680 triplet states, which decay with a 1 ms lifetime [9]. This means that the incident light intensity gives a steady-state triplet population of less than 2%, of the reaction centres present in the illuminated volume of 0.1 ml. Stirring of the sample reduces this proportion further. Less than 1 in 10^4 of the reaction centres in the illuminated volume are excited by each pulse.

All errors are quoted as one standard deviation.

Analysis

Lifetimes were calculated by iterative re-convolution based on the Marquardt fitting algorithm [16], assuming multi-exponential decay kinetics. The quality of the fits was judged using a reduced χ^2 criterion and plots of the weighted residuals. All of the fluorescence decays from intact D1/D2 samples were best represented by a sum of four exponentials. Decays from samples with Q_y band absorption maxima below 673 nm were best represented by a two-exponential model.

It has previously been established that at 277 K, 85% of the D1/D2 fluorescence is due to the sum of the charge-recombination component, and a 6.5 ns component which is assigned to chlorophyll that is energetically uncoupled from the process of charge separation [3]. The remaining emission is due to two components of approx. 1.5 ns and 100 ps. All the decays were measured on a scale of 180 ps per channel, over 512 channels. This helps to establish the value of the long lifetime more accurately than using a shorter scale. The time per channel used for data collection means that the lifetimes for the two short decays cannot be accurately established, although measurements on this timescale will approximately indicate the relative initial ampli-

tudes of these two components. No detailed interpretation can be attached to the short lifetimes in this analysis, although they may genuinely represent additional fluorescence decays from active reaction centres.

The amplitudes and lifetimes of the longest component were found to vary little between χ^2 values from 1.1 to 2.0. A random distribution of the residuals over the latter part of the decay (after the laser pulse), indicated that the model satisfactorily represented the two longest components. When poor χ^2 values were obtained, they were found to be due to a non-random distribution of the residuals over the first few channels of the decay only, and this had little effect on the values found for the two longer components.

All decays were analysed both with all parameters free running, and also by fixing the value for the lifetime assigned to the energetically uncoupled chlorophyll. The uncoupled chlorophyll lifetime was fixed at three separate values, in order to determine the effect that variation in this lifetime would have on the extraction of the recombination fluorescence parameters by the curve fitting procedure. Fixed values chosen were 5 ns, 6.5 ns and 8 ns.

All yields of fluorescence components are quoted as the time integral of the appropriate component of the fluorescence decay.

Results

Experimental spread

The experimental errors in both the yield and lifetime of the charge-recombination component were determined from the spread of measurements on different samples from the same batch, at 277 K. The relative fluorescence yield of this component was $(45.4 \pm 2.4)\%$, and the lifetime was (36.8 ± 2.0) ns. Measurements on samples from different batches showed a greater variation in the yield of the recombination fluorescence, $(44.5 \pm 4.0)\%$; while the variation in the long lifetime between batches was found to be the same as that within a batch; the value obtained was (37.0 ± 2.0) ns.

The eluant from the final column was also collected in 1 ml fractions. A study of these column fractions (data not presented) indicated a systematic variation in the value obtained for the yield of the recombination component. The yields found for the first two fractions from the column (43.9% and 43.0%) were the lowest. The average value for the yield of the remaining fractions was $(49.9 \pm 1.4)\%$. The lifetimes found for the recombination component did not show a systematic variation, the average being (37.4 ± 1.1) ns.

The spread of data within a batch probably indicates the precision of the SPC experiments, while that between batches shows a genuine variation in sample heterogeneity.

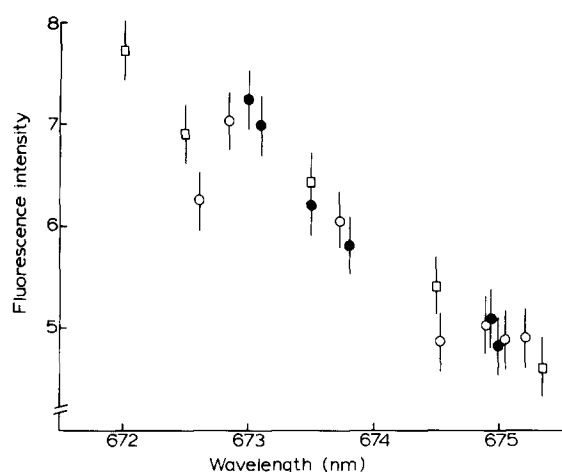


Fig. 2. The steady-state fluorescence intensity of D1/D2 reaction centres, under aerobic conditions at a chlorophyll concentration of $2 \mu\text{g} \cdot \text{ml}^{-1}$, as a function of the Q_y band absorption maximum. The fluorescence intensity is the integral of the fluorescence band and is in arbitrary units. The wavelength shifts of the absorption maximum to the blue were caused either by exposure to light at 277 K (\circ), to a temperature of 295 K in the dark (\bullet) or by the addition of 1% Triton X-100 to the buffer (in the dark at 277 K) (\square).

Damaged reaction centres

Intact D1/D2 samples showed Q_y absorption and fluorescence maxima of $(675.9 \pm 0.2) \text{ nm}$ and $(682.5 \pm 0.5) \text{ nm}$, respectively. Blue-shifts in these Q_y absorption and fluorescence maxima were induced by exposing the samples (under aerobic conditions) either to light at 277 K, to a temperature of 297 K in the dark, or to different concentrations of Triton X-100 (in the dark at 277 K). Samples which had been exposed to light had steady-state absorption maxima of approx. 672 nm after 30 min, while those exposed to heat showed a similar absorption change after 36 h. Samples with 0.2% Triton X-100 in the buffer showed an absorption maximum below 673 nm after 3 h, but those with 1% Triton X-100 took only 45 min to reach this stage.

As the Q_y band absorption maximum shifts to the blue, the steady-state fluorescence intensity of D1/D2 samples increases; this is shown in Fig. 2. This increase in the fluorescence yield is also accompanied by a blue shift in the emission peak.

Table I shows the effect that damaging the reaction centres has on the time-resolved fluorescence. As the steady-state absorption and fluorescence maxima shift to the blue, the yield of the recombination fluorescence decreases, while that of the uncoupled chlorophyll component increases and the sample becomes more fluorescent overall (see Fig. 2). When the sample shows an absorption maximum of 670.0 nm, 98% of the fluorescence is due to uncoupled chlorophyll with a 6.3 ns lifetime. This indicates that one of the effects of damaging the complex is to decouple chlorophyll from the charge-separation reaction. Damaging the reaction centres by the methods described above results in 'inac-

tive' [10] samples. Samples which show a Q_y band absorption maximum less than 673 nm are termed inactive. Fluorescence decays from these inactive samples are best represented by a sum of two exponentials with at least 90% of the emission coming from uncoupled chlorophyll.

The isolated reaction centre complex is susceptible to light damage, even when most of the oxygen has been removed [3]. To reduce the effect of light induced damage samples were only exposed to 5 min of laser light during the SPC data collection. Indeed, if the exposure of anaerobic samples was extended to 10 min, at 277 K, the yield of the charge-recombination component fell by $(8.9 \pm 0.6)\%$ while the lifetime was reduced by $(6.6 \pm 0.8) \text{ ns}$. The Q_y band absorption peak shifted from $(675.9 \pm 0.2) \text{ nm}$ to $(675.8 \pm 0.2) \text{ nm}$.

Quantum yields of fluorescence components at 277 K

The calculation of the quantum yield of the charge-recombination fluorescence assumes that all of the 6.5 ns component observed in D1/D2 samples is due to uncoupled chlorophyll (see Discussion) which has the same fluorescence quantum yield as monomeric chlorophyll *a* in diethyl ether, 0.32 [17]. The fluorescence quantum yield of monomeric chlorophyll *a* in solution hardly varies with solvent [17]. Chlorophyll *a* in ether exhibits a lifetime of 6.7 ns [15], which is similar to the lifetime of the uncoupled chlorophyll present in D1/D2 samples. This suggests that the chlorophyll in these different conditions will have similar fluorescence quantum yields.

The relative steady-state fluorescence yields of the intact D1/D2 complex and of monomeric chlorophyll *a* in ether were measured at 277 K. Both samples had a chlorophyll concentration of $10 \mu\text{g} \cdot \text{ml}^{-1}$ and were excited at 405 nm, where they had the same optical absorbance. The fluorescence yields were obtained by integrating over the fluorescence bands, chlorophyll in either was found to be (8.5 ± 0.4) -times as fluorescent

TABLE I

Time-resolved fluorescence measurements on intact and damaged D1/D2 reaction centres

λ_{abs} and λ_{flu} are the Q_y band absorption and fluorescence maxima, respectively. τ_1 is the lifetime and F_1 the relative yield of the charge-recombination fluorescence component. τ_2 and F_2 are the corresponding values for the 6.5 ns fluorescence component. * indicates that the curve fitting procedure could not detect the presence of a component with a lifetime longer than 6.5 ns. The fluorescence decay curves with Q_y band absorption maxima at 672.9 nm and 670.0 nm were best represented by a two-exponential model.

λ_{abs} (nm)	λ_{flu} (nm)	τ_1 (ns)	τ_2 (ns)	% F_1	% F_2
675.9	682.5	36.5	6.5	44	40
672.9	678.0	*	6.2	*	90
670.0	673.0	*	6.3	*	98

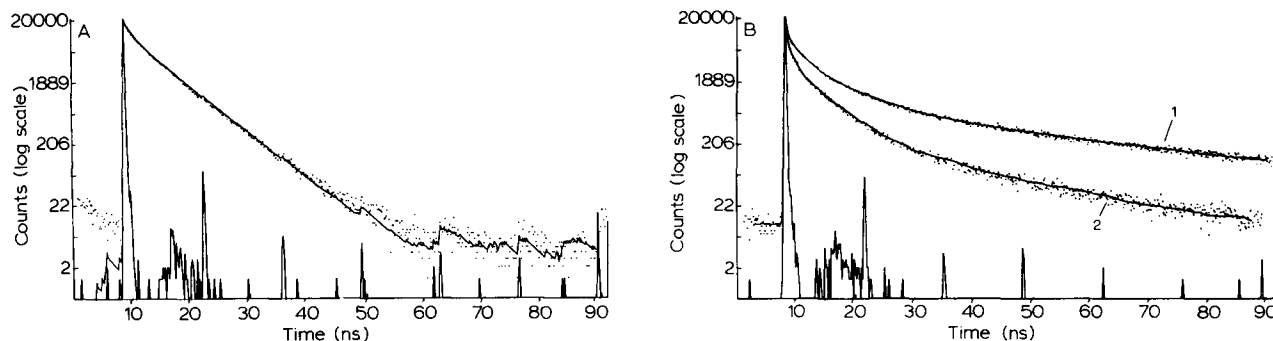


Fig. 3. The effect of the addition of 25 μM DBMIB to D1/D2 cytochrome *b*-559 reaction centres, at 277 K. (A) shows the fluorescence decay of an inactive sample, with a Q_y band absorption maximum at 672.9 nm, before the addition of the quinone. After the addition of 25 mM DBMIB there was no change to the fluorescence decay. Both decays are best represented by a sum of two exponentials with 90% of the fluorescence resulting from a component with a lifetime of 6 ns and the remainder being due to a component with a lifetime of approx. 1 ns. In (B) curve (1) shows a typical fluorescence decay of an intact D1/D2 sample, with a Q_y band absorption maximum of 675.9 nm, before the addition of DBMIB. Analysis of this decay gives a 44% yield of a 37 ns lifetime and a 40% yield of a 6.5 ns lifetime. Curve (2) is the fluorescence decay of an intact sample containing 25 μM DBMIB. Analysis of this decay gives a 21% yield of a 23 ns lifetime and a 46% yield of a 6 ns lifetime. This sample had not previously been exposed to laser light. Both curves (1) and (2) were best represented by the sum of four exponentials. The instrument response is shown below the decay curves.

as the D1/D2 sample. The fluorescence quantum yield of D1/D2 samples is found to be (0.040 ± 0.003) . However, 40% of the fluorescence from D1/D2 samples is due to contaminant uncoupled chlorophyll, while 44% is due to charge recombination. Therefore the fluorescence yield due to the charge recombination can be estimated to be (0.020 ± 0.002) at 277 K.

The relative fluorescence yield of the uncoupled chlorophyll suggests that it constitutes only 6% of the total chlorophyll present and this means that 94% of the chlorophyll in an active sample is associated with charge separation.

The shortest lifetime obtained from the fits was (0.1 ± 0.1) ns [3], the absolute quantum yield for this component is approx. 0.05. If this component is assigned to prompt fluorescence then it should have a lifetime of 3 ps, equal to the rate of charge separation [8]; the lifetime we observe is limited by the time resolution of the experiment. Using 19 ns as the natural lifetime of P680 (see Discussion) and a lifetime of 3 ps the theoretical value for the absolute quantum yield of the prompt fluorescence is $1.6 \cdot 10^{-4}$. However the initial amplitude of the 0.1 ns lifetime we observe is dominated by scattered light so the quantum yield obtained for this component is two orders of magnitude greater than the theoretical value. Since the decays were taken on a scale of 180 ps per channel, giving 92 ns full scale, the lifetimes and amplitudes of the two longer components (6.5 ns and 37 ns) are unaffected by this scatter, since this occurs over a much shorter timescale. The initial amplitudes of the longer components, which result from the analyses, are effectively extrapolated from a region of the decay curve where there is no scatter present.

Addition of quinone to the reaction centres at 277 K

The effect of adding the quinone DBMIB was investigated. The quinone concentration of the stock solution in ethanol was altered between 100 mM and 2 mM. In each experiment only 1 μl of the stock solution was added to 2 ml of sample, to give DBMIB concentrations between 50 μM and 1 μM . This was to minimise the amount of ethanol added to the samples. The addition of 1 μl of ethanol to 2 ml of D1/D2 sample had no effect on the time-resolved fluorescence.

Addition of DBMIB at a concentration of 25 μM to an inactive D1/D2 sample has very little effect on the total fluorescence yield. The inactive sample was pre-

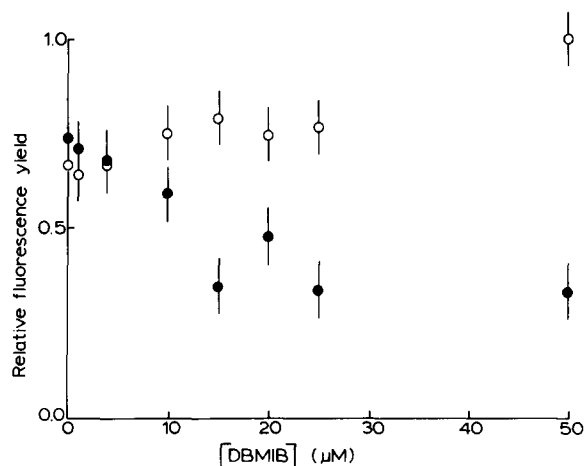


Fig. 4. The relative fluorescence yields of the charge-recombination fluorescence component (\bullet) and the 6.5 ns component (\circ) from active samples as a function of the concentration of DBMIB. Separate samples were used for each DBMIB concentration. The relative yields are from analyses in which the 6.5 ns lifetime was fixed.

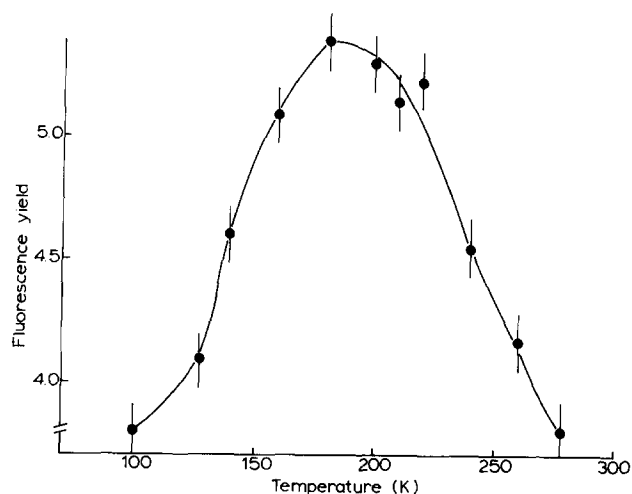


Fig. 5. The total fluorescence yield of an active D1/D2 reaction centre as a function of temperature. The yield is the integral of the fluorescence band in arbitrary units.

pared by subjecting a fresh sample to laser excitation under aerobic conditions. After this the sample had a Q_y absorption maximum at (672.9 ± 0.2) nm and a 6.2 ns lifetime represented 90% of the fluorescence. After the addition of DBMIB to this sample, 90% of the fluorescence had a 6.0 ns lifetime (see Fig. 3a). Addition of 25 μ M DBMIB was also found to have no effect on the fluorescence yield of 10 μ g \cdot ml $^{-1}$ chlorophyll *a* in ethanol (data not presented).

Addition of 25 μ M DBMIB to active undamaged D1/D2 samples results in a decrease in both the amplitude and lifetime of the 37 ns component, as shown in Fig. 3b, with much less effect on the 6.5 ns component. Fig. 4 shows that as the concentration of DBMIB is increased, the relative yield of the 37 ns component decreases and that of the 6.5 ns component increases. The presence of 25 μ M of DBMIB reduced the total fluorescence yield of active samples by approx. 50%.

Temperature effects on the fluorescence from the reaction centres

The addition of glycerol to the samples had no effect on the position of the Q_y band absorption maximum, or on the yield of the recombination fluorescence. A 36.5 ns fluorescence component was shown to contribute 40% of the total emission of the D1/D2 particle in a buffer containing 80% glycerol at 277 K. Cooling and subsequent thawing of the samples did not affect their activity. All active samples had Q_y band absorption maxima at (675.9 ± 0.2) nm both before and after all SPC measurements.

The effect of temperature on the steady-state fluorescence yield of an active D1/D2 sample is shown in Fig. 5. The fluorescence peak of the D1/D2 sample was (682.5 ± 0.5) nm at all temperatures. From Fig. 5 it can be seen that the steady-state fluorescence yield of an intact D1/D2 sample increases as the temperature is lowered to 180 K and then falls as the temperature is

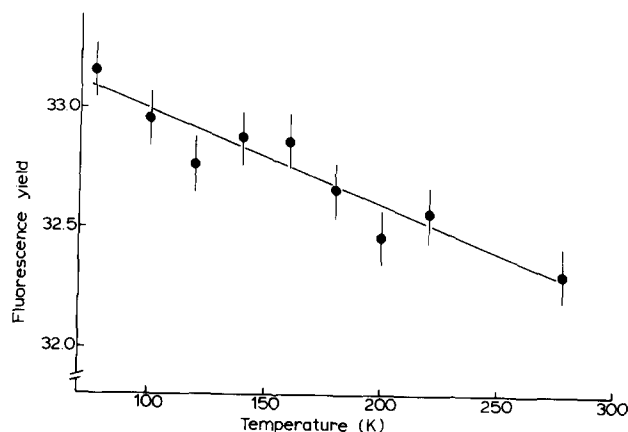


Fig. 6. The total fluorescence yield of an inactive D1/D2 sample, with a Q_y band absorption maximum at 670 nm, as a function of temperature. The intensity scale is the same as in Fig. 5.

further decreased to 100 K. This effect is also seen in the temperature dependence of the total fluorescence yield observed for *Rhodobacter sphaeroides* reaction centres [18], which have a fluorescence maximum at around 200 K.

Fig. 6 shows the change in fluorescence yield with temperature for an inactive D1/D2 sample, with a Q_y band absorption maximum of (670.0 ± 0.2) nm and a fluorescence maximum of (673.0 ± 0.5) nm. The intensity scale is the same as in Fig. 5. The change in yield is monotonic, and less than that in active samples (see Fig. 5). SPC data from this sample indicated that approx. 98% of the fluorescence had a 6.3 ns lifetime.

From the time-resolved fluorescence data and the charge-recombination fluorescence quantum yield, it is possible to calculate the equilibrium constant and the free-energy difference for the $(P680^* \rightleftharpoons P680^+ Ph^-)$ equilibrium (see Discussion); these were determined over the temperature range 77 K to 277 K.

Table II presents the results of time-resolved fluorescence measurements obtained over the range 77 K to

TABLE II

Fluorescence decay kinetics and $\Delta G(P680^+ Ph^- - P680^*)$ values for D1/D2 reaction centres over the temperature range 277 K to 77 K

τ_1 , F_1 and ϕ_1 are the charge-recombination fluorescence lifetime, relative yield and quantum yield, respectively. F_2 is the relative yield of the 6.5 ns fluorescence component. K is the equilibrium constant for the $(P680^* \rightleftharpoons P680^+ Ph^-)$ equilibrium and ΔG is $\Delta G(P680^+ Ph^- - P680^*)$. T is the temperature at which the values are determined.

T (K)	τ_1 (ns) ± 2.0	% F_1 ± 4.0	F_1/F_2 ± 0.08	ϕ_1 ± 0.002	K ± 12.8	$-\Delta G$ (eV) ± 0.003
277	37.5	47.8	1.20	0.020	98.7	0.110
200	33.9	39.6	1.02	0.019	93.9	0.078
180	34.1	34.6	0.94	0.018	102.6	0.072
127	39.4	31.8	0.94	0.018	116.5	0.052
100	36.1	27.6	0.93	0.018	106.7	0.040
77	40.5	9.0	0.49	0.010	222.0	0.036

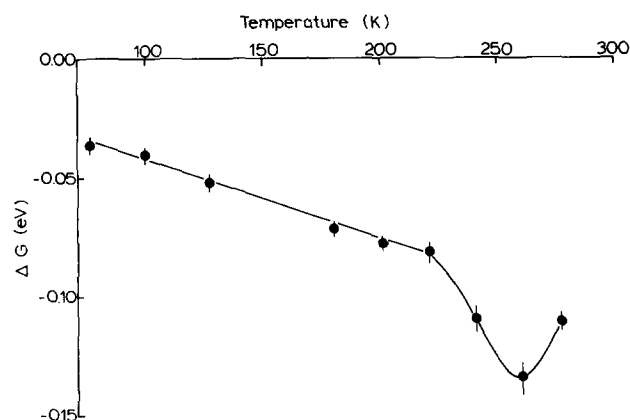


Fig. 7. $\Delta G(\text{P680}^+ \text{Ph}^- - \text{P680}^*)$ in intact D1/D2 reaction centres as a function of temperature.

277 K. Also shown are the values for the lifetime, τ_1 , and quantum yield, ϕ_1 , of the recombination fluorescence, the equilibrium constant for the $(\text{P680}^* \rightleftharpoons \text{P680}^+ \text{Ph}^-)$ equilibrium, K , and free-energy difference between P680^* and the radical pair, $\Delta G(\text{P680}^+ \text{Ph}^- - \text{P680}^*)$. The results shown in Table II are those from analysis of the data with the uncoupled chlorophyll lifetime fixed at 6.5 ns during the fits. Free-running fits gave similar results. The χ^2 values varied between 1.1 to 1.8. Analysing the data by fixing the uncoupled chlorophyll lifetime at 8.0 ns or 5.0 ns altered the value obtained for the free-energy change by only 4%.

An increase is observed in the relative fluorescence yield of the shortest component as the temperature is decreased from 277 K to 77 K (data not presented). This is due mainly to an increase in the amount of scattered light as the sample is frozen.

There is no clear correlation between the change in the relative yield of any fluorescence component with

temperature (see Table II) and that of the overall fluorescence yield (see Fig. 5). This implies that the origins of the fluorescence components are not affected by temperature but that the rates of non-radiative processes are changing. This has the effect of reducing the number of singlet states as a whole.

Fig. 7 shows the variation of $\Delta G(\text{P680}^+ \text{Ph}^- - \text{P680}^*)$ with temperature. The free-energy gap is negative over the temperature range and decreases linearly with temperature between 220 K and 77 K. Between 220 K and 277 K the ΔG curve is nonlinear, with a maximum ΔG value occurring at approx. 260 K. In Fig. 8 this free-energy curve is compared to results obtained by Woodbury and Parson [18] for the corresponding free-energy change in *Rb. sphaeroides* reaction centres (with chemically reduced ubiquinone).

Discussion

The assignment of the decay kinetics described below confirms the assignment of the 37 ns component to charge recombination, and also that the 6.5 ns component is not connected with this process. This assignment of the decay kinetics allows the equilibrium constant and the free-energy difference between P680^* and $\text{P680}^+ \text{Ph}^-$ to be calculated. The temperature dependence of the free-energy difference allows the enthalpy and entropy contributions to be determined.

Assignment of the fluorescence decay kinetics at 277 K

The 37 ns and 6.5 ns fluorescence components can be shown to be independent of each other by damaging reaction centres and by monitoring the effect of adding the quinone DBMIB.

The effect of damaging reaction centres

It has already been established that aerobic samples at 277 K are unstable when subjected to dye laser excitation [3]. Damaged samples lose the 37 ns component and this is accompanied by a significant increase in the yield of the 6.5 ns component. A shift in both the steady-state absorption and fluorescence maxima to the blue accompanies the loss of the 37 ns component (see Table I). Fig. 2 shows that the steady-state fluorescence intensity of the D1/D2 complex progressively increases as the sample is damaged. This increase in the yield of the 6.5 ns component has already been reported [3,6], and it is accompanied by an increase in the total fluorescence intensity of the D1/D2 sample. This is consistent with the assignment of the 6.5 ns lifetime to chlorophyll which is not coupled to charge separation. The uncoupled chlorophyll has a much greater fluorescence quantum yield (approx. 0.32), than the D1/D2 sample which has a fluorescence quantum yield of approx. 0.04. It is therefore expected that, as the amount

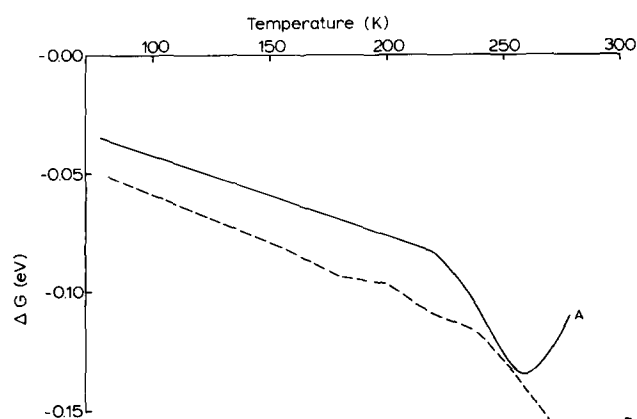


Fig. 8. Comparison of the temperature dependence of the free-energy gap between the excited special pair and the primary radical pair in PS II and bacterial reaction centres. Curve A is the $\Delta G(\text{P680}^+ \text{Ph}^- - \text{P680}^*)$ curve for D1/D2 reaction centres, as shown in Fig. 7. Curve B is that obtained by Woodbury and Parson, for the corresponding free-energy change in *Rhodospirillum rubrum* (with chemically reduced ubiquinone), with 7.3 μM reaction centres in 0.005% Triton X-100.

of uncoupled chlorophyll in the sample increases, the overall fluorescence intensity of the D1/D2 sample will also increase and Fig. 2 shows this to be the case. Concomitant with this is the loss of the 37 ns lifetime component, which reflects a reduction in the fluorescence due to charge recombination. This could be due to the increased competition by other deactivation pathways (after charge separation), or it could indicate that charge separation does not occur.

The amount of uncoupled chlorophyll present in D1/D2 samples is related to the absorption maximum of the sample. A comparison of Figs. 5 and 6 at 277 K shows that a sample with an absorption maximum of 670 nm is more fluorescent than an intact sample (with a maximum at 676 nm) by a factor of approx. 8. This is consistent with the uncoupled chlorophyll having similar fluorescent properties as monomeric chlorophyll *a* in diethyl ether, since the latter is 8.5-times as fluorescent as an intact D1/D2 sample (see Results). The data presented in Fig. 2 seem to contradict this; a sample with an absorption maximum at 672 nm is only approximately twice as fluorescent as an intact sample. However, for absorption maxima below 672 nm the increase in the fluorescence intensity of the samples is no longer linear with wavelength (Booth, P.J., unpublished data). Samples with absorption maxima of 670 nm are approx. 6- to 8-times as fluorescent as intact samples.

The origin of the 6.5 ns component may be heterogeneous; there could be contributions other than chlorophyll uncoupled from the charge-separation process. One possibility is that it may arise from dimer chlorophylls, with different natural lifetimes and therefore different fluorescence quantum yields. Another contribution could be from charge-recombination fluorescence from radical pairs which exhibit a 6.5 ns lifetime, possibly from damaged reaction centres, or from equilibration of singlet and triplet radical pairs on this timescale. However, these processes are unlikely to contribute significantly to this component, most dimers tend to show shorter fluorescence lifetimes than monomers therefore dimer chlorophylls are likely to show lifetimes less than 6.5 ns. The effect of addition of quinone to the reaction centres, described in the next section, suggests that the 6.5 ns component is unconnected with charge-recombination.

Higher plant complexes which have been studied by SPC consistently show a variable amount of a component with a lifetime of approx. 6 ns. Lifetimes of 5.5–6.5 ns have been assigned to unquenched chlorophyll *a* bound to protein in isolated Photosystem I reaction centre preparations [19], to free chlorophyll *a* in detergent micelles, in samples of the major light-harvesting complex of PS II (LHCII) in conditions of high detergent [15] and to chlorophyll energetically uncoupled from the process of charge separation in Photo-

system II (PS II) core preparations, with approx. 20 chlorophyll *a* molecules per cytochrome *b*-559 (Crystall, B. and Booth, P.J., unpublished data). The amount of this component (with a lifetime of approx. 6 ns) present in the samples has also been found to depend on the treatment of the sample, in the case of the LHCII and PS II core samples the yield of this component depended on the type and concentration of detergent. The 6.5 ns component observed in D1/D2 samples is therefore probably dominated by fluorescence from chlorophyll which is uncoupled from the charge-separation process and exhibits photophysical properties similar to that of monomeric chlorophyll *a* in ether. This chlorophyll is likely to be monomeric and either in a protein environment or a detergent micelle.

The effect of the addition of quinone to the reaction centres

Quinones are known to quench chlorophyll fluorescence, and 16 mM duroquinone has been found to reduce the fluorescence of 3 μ M chlorophyll *a* in ethanol by half [20]. We find that the low concentration of DBMIB (25 μ M) used for the experiments described in this paper is insufficient to quench fluorescence from isolated chlorophyll in ethanol. The fluorescence from inactive D1/D2 samples is also unaffected by this concentration of DBMIB. In active reaction-centre samples, the 6.5 ns component is essentially unaffected by the addition of quinone; however, the addition of 25 μ M quinone reduces both the lifetime and amplitude of the 37 ns component. The different degrees of quenching of the two fluorescence components suggests these components originate from two different processes. Quinone might be expected to accept an electron from the reduced pheophytin of the radical pair, and so prevent charge recombination. However, although the data discussed above can be explained by this mechanism, they do not prove that the quinone is accepting an electron from the reduced pheophytin. The observed quenching of the ($P680^* \rightleftharpoons P680^+Ph^-$) equilibrium may be due to some trivial mechanism. Nevertheless, the reduction in the lifetime of the recombination fluorescence on the addition of quinone is consistent with the idea that the quinone is providing an additional deactivation pathway from this equilibrium. This suggests that of the two lifetimes, only the 37 ns component is due to charge recombination.

Sample heterogeneity

The results obtained from the individual column fractions indicate that the relative yields of the charge-recombination and uncoupled chlorophyll components vary systematically with position on the column. This suggests that there is some heterogeneity in the samples due to variations in the amount of uncoupled chlorophyll present. The fractions which come from the lead-

ing edge of the chromatographic peak have a higher yield of the 6.5 ns component, and this may be due to the presence of small amounts of contaminant polypeptides in this part of the column or to a higher proportion of damaged reaction centres. This suggests that the uncoupled chlorophyll may actually be bound to the protein to some degree.

In summary, the 6.5 ns component is assigned to chlorophyll which plays no role in the process of charge separation. The 37 ns component is due to fluorescence from P680* which is formed by charge recombination of the primary radical pair, P680⁺Ph⁻, a concept originally proposed by Klimov et al. [21]. The physical origins of these two fluorescence components are independent of each other.

$$\Delta G(\text{P680}^+ \text{Ph}^- - \text{P680}^*)$$

Time-resolved measurements indicate that the decay kinetics assigned to P680* are predominantly mono-exponential, with a lifetime of 37 ns. This suggests that an equilibrium has been established between P680* and the radical pair. The equilibrium constant, K , between P680* and the radical pair can be shown to be related to observable parameters as follows,

$$K = \frac{[\text{P680}^+ \text{Ph}^-]_e}{[\text{P680}^*]_e} = \frac{\tau_1}{\phi_1 \tau_0} \quad (1)$$

where τ_1 is the lifetime of the recombination fluorescence, τ_0 is the natural lifetime of P680* and ϕ_1 is the quantum yield of recombination fluorescence. The equilibrium concentration of P680*, $[\text{P680}^*]_e$, can be found from the initial amplitude of the recombination fluorescence. The (P680* \rightleftharpoons P680⁺Ph⁻) equilibrium strongly favors the charge-separated state. It is therefore possible to calculate the concentration of the radical pair at equilibrium, $[\text{P680}^+ \text{Ph}^-]_e$, from the theoretical initial amplitude of fluorescence from P680*.

The equilibrium constant can therefore be calculated from the quantum yield (ϕ_1) and lifetime (τ_1) of the recombination fluorescence, and the natural lifetime of P680* (τ_0). $\Delta G(\text{P680}^+ \text{Ph}^- - \text{P680}^*)$ can then be calculated using the expression

$$\Delta G = -k_B T \ln K, \quad (2)$$

where k_B is the Boltzmann constant. This gives an equilibrium constant of (98.7 ± 12.8) and a ΔG value of $-(0.110 \pm 0.002)$ eV, at 277 K.

The accuracy of ΔG

The natural lifetime of P680* is taken as that of chlorophyll *a*, which is approx. 19 ns [22]. It is conceivable that a chlorophyll dimer will have a shorter natural lifetime. The logarithmic relationship between

ΔG and K (Eqn. 2) means that the determination of the free energy is relatively insensitive to the value used for the natural lifetime of P680*, as long as it is of the order of tens of nanoseconds. Taking the natural lifetime as 8.5 ns instead of 19 ns only introduces a 10% increase in the ΔG value. The natural lifetime for P680* has recently been estimated using transient absorption spectroscopy [9], and was found to be of the order of 19 ns. The natural lifetime was assumed to be temperature-independent.

Analysis of the fluorescence decay data with the uncoupled chlorophyll lifetime fixed to 5 ns or 8 ns changed the ΔG value by only 4%. This also indicates the insensitivity of the ΔG value to variations in the value of this lifetime. However, the uncoupled chlorophyll lifetime is unlikely to differ from 6.5 ns by even as much as 1.5 ns when the temperature is lowered to 77 K. The lifetime of monomeric chlorophyll in ethanol changes only from (6.3 ± 0.1) ns, at 298 K to (6.2 ± 0.1) ns at 77 K [23].

Some uncertainty in ΔG also comes from uncertainties in the charge-recombination fluorescence quantum yield and lifetime (ϕ_1 and τ_1 in Table II), giving a $\Delta G = -(0.110 \pm 0.003)$ eV, at 277 K. However, the dominant contribution to the uncertainty in ΔG is that of the natural lifetime of P680*, at most this could change ΔG from -0.11 eV to -0.12 eV, at 277 K.

Determination of the recombination fluorescence quantum yield, ϕ_1

The quantum yield for the recombination fluorescence (ϕ_1) from the D1/D2 particle at temperatures below 277 K was calculated by using the quantum yield of fluorescence of the uncoupled chlorophyll as an internal marker, and by noting the relative fluorescence yields of the uncoupled chlorophyll and charge-recombination components of the fluorescence decays. The fluorescence quantum yield of the uncoupled chlorophyll was taken as 0.32 (see Results). Fig. 6 shows that the fluorescence yield of an inactive D1/D2 particle increases linearly as the temperature is decreased. The fact that most of the emission is due to a 6.3 ns lifetime suggests that most of the chlorophyll in this sample is essentially monomeric, either in a protein environment or possibly free from the protein. These results indicate that the fluorescence yield of the uncoupled chlorophyll present in the active D1/D2 samples may vary with temperature in a similar way to that shown in Fig. 6. This temperature dependence of the uncoupled chlorophyll fluorescence quantum yield was included in our calculations of ϕ_1 .

Enthalpy and entropy contributions to ΔG

Fig. 7 shows that the free-energy difference between P680* and the radical pair has a linear dependence on temperature from 220 K to 77 K. Using the expression

$\Delta G = \Delta H - T\Delta S$ over this region allows values for ΔH , the enthalpy change associated with the charge-separation step, and for ΔS , the accompanying entropy change, to be determined. The enthalpy difference is found from the intercept at 0 K to be $-(5.0 \pm 0.3) \cdot 10^{-3}$ eV and the entropy change is the gradient, $+(3.8 \pm 0.3) \cdot 10^{-4}$ eV \cdot K $^{-1}$. This indicates that the free-energy difference is dominated by the entropy contribution. (At 200 K, $\Delta G \cong -T\Delta S = -(7.6 \pm 0.2) \cdot 10^{-2}$ eV.)

The free-energy difference shows a nonlinear temperature dependence in the region 220 K to 277 K. This may be because either the entropy difference is temperature-dependent over this range or the enthalpy difference becomes significant and also temperature-dependent. It was difficult to obtain data with high signal-to-noise ratio in this region, as the fluorescence yield of the D1/D2 sample dropped significantly when the sample was exposed to laser light. This was not observed either at 277 K or below 220 K. Therefore the errors in the ΔG values are larger in the nonlinear region.

Comparison of Photosystem II and purple bacteria

Fig. 8 shows the variation of the free-energy difference between the excited bacteriochlorophyll special pair, P^* , and the primary radical-pair state, $\Delta G(P^+BPh^-P^*)$ as determined by Woodbury and Parson for isolated reaction centres from *Rb. sphaeroides* (with chemically reduced ubiquinone) [18]. This is remarkably similar to the temperature dependence for the corresponding free energy change discussed in this paper for higher plant PS II reaction centres (Fig. 8). The entropy change for the bacterial reaction centre is $-6.5 \cdot 10^{-4}$ eV \cdot K $^{-1}$ (for 7.3 μ M reaction centres in 0.005% Triton X-100). In addition, the temperature dependence of the free energy is nonlinear over approximately the same region. The authors observed that this nonlinearity was dependent on the concentration of Triton X-100 in the buffer. The ΔG curve for the *Rb. sphaeroides* reaction centre is displaced vertically from that of the D1/D2 particle, indicating a larger enthalpy difference.

The free energy difference between the excited special pair and the primary radical pair is dominated by the entropy change from 77 K to 200 K in both the D1/D2 reaction centre and in *Rb. sphaeroides*. This appears to disagree with results obtained from studies of the magnetic field dependence of the triplet decay kinetics in quinone-depleted *Rb. sphaeroides* reaction centres [24,25]. These conclude that $\Delta G(P^+BPh^-P^*)$ in quinone-depleted *Rb. sphaeroides* reaction centres is dominated by the enthalpy change. However, their measurements were made only over the range 185 K to 290 K, which corresponds to the nonlinear region of ΔG for both D1/D2 and *Rb. sphaeroides*. This suggests that this nonlinearity may be due in part to an enthalpy contribution. The conditions of the samples were also not the same as in the study by Woodbury et al. [18],

the ubiquinone had been removed instead of chemically reduced and the concentration of the detergent in the buffer was higher, being 0.1% Triton X-100 in Ref. 25.

The presence of quinone in the reaction centres may affect the energy of the radical pair. Woodbury et al. [26] have measured $\Delta G(P^+BPh^-P^*)$ to be -0.148 eV in quinone-depleted *Rb. sphaeroides* reaction centres, and -0.168 eV in quinone-reduced reaction centres, at 295 K. In contrast Hörber et al. [27] determine these free energies to be $-(0.23 \pm 0.01)$ eV in the reduced, and $-(0.26 \pm 0.01)$ eV in the quinone-free case. They obtain similar values for *Rhodospseudomonas viridis*. However, Woodbury et al. [18,26] and Hörber et al. [28] used different kinetic models in their analyses. The fluorescence from the bacterial reaction centres consists of three components, of approx. 0.5 ns, 2 ns and 12 ns. Hörber et al. propose that a proportion of the initial charge separation occurs along the M branch as well as the L branch [27–29] (the dominant path of the electron transfer [30]). The longest lifetime and the -0.26 eV free-energy change is assigned to charge-recombination fluorescence due to the radical pair on the L branch and the 2 ns lifetime to recombination fluorescence from the M branch. The free-energy gap in the M branch is calculated to be $-(0.13 \pm 0.01)$ eV in both *Rb. sphaeroides* and *Rps. viridis*. Woodbury et al. only consider electron transfer down one branch and calculate the free-energy gap from the initial amplitudes of all three of the fluorescence components.

The model invoked by Hörber et al. for both *Rb. sphaeroides* and *Rps. viridis* in terms of parallel electron transfer along the L and M branches gives a branching ratio for the primary electron transfer rates, $k_L/k_M = 6$ for reaction centres lacking ubiquinone, or approx. 3 for centres with reduced ubiquinone, at 295 K [28] (where k_L and k_M are the primary electron-transfer rates along the L and M branches, respectively). Recent transient absorption measurements have indicated branching ratios, $k_L/k_M \approx 200$, for *Rps. viridis* reaction centres at 90 K [31] and $k_L/k_M \geq 25$ for *Rb. sphaeroides* reaction centres at 80 K [32]. Since the rates of primary electron transfer in *Rb. sphaeroides* and *Rps. viridis* reaction centres increase only by factors of approx. 2 and 4, respectively, from 295 K to 80 K [33], it is likely that these branching ratios are similar to those at 295 K. These measurements therefore suggest that at low temperatures (and possibly at higher temperatures) electron transfer along the M branch does not compete significantly with that along the L branch. This suggests that charge separation and subsequent recombination along the M branch does not contribute to the fluorescence kinetics.

If the results of Hörber et al. are interpreted more generally than in the specific case of parallel electron transfer along the two branches then the free-energy value of -0.23 eV for the initial charge-separation

reaction corresponds to a relaxed radical-pair state [24]. Analysis of the data obtained by Woodbury et al. using only the longest fluorescence lifetime also yields a free-energy value of -0.25 eV, in good agreement with that obtained by Hörber et al. The magnetic data [25] also give a free energy of -0.263 eV, which is consistent with the above. Woodbury et al. [18] obtain a free-energy value of -0.16 eV, it has been suggested that this corresponds to a non-relaxed radical-pair state [18,24].

The multiexponential decay kinetics of the delayed fluorescence observed from bacterial reaction centres have not been unambiguously assigned. It is likely that there is some contribution from nuclear relaxations of the radical pair on a nanosecond timescale, as proposed by Woodbury et al. [18]. This model has also been found to be consistent with recent measurements of the triplet quantum yield and decay kinetics, and delayed fluorescence at very high magnetic fields [34]. The apparent contradiction of the fluorescence data and the magnetic data in terms of the entropy contribution to $\Delta G(P^+BP^--P^*)$ does not appear to have been resolved. However, great caution has to be taken when comparing results from samples under different conditions, particularly between reaction centres with reduced quinone and those where the quinone has been removed (as pointed out by Ogrodnik et al. [24]) and with respect to temperature and detergent concentration.

The analysis of fluorescence data from the D1/D2 complex discussed in this paper for the calculation of the free-energy gap between $P680^*$ and the radical pair, is comparable to the method of Hörber et al. Only the initial amplitude of the longest fluorescence component was used to determine the free-energy change. This method of analysis is independent of the model invoked to explain the shortest lifetimes observed in the fluorescence kinetics. The results suggests that, in PS II the free-energy gap of -0.11 eV, at 277 K, between the excited special pair and the radical pair is approximately half that in the bacterial reaction centre.

Particularly good sequence homologies exist between the D1 and D2 polypeptides of PS II and the L and M subunits of purple bacteria [35–37]. The PS II reaction centre is expected to show roughly the same symmetry as that of purple bacteria. The D1 polypeptide is thought to correspond to the L subunit and the D2 to the M subunit. By analogy with the bacterial case, the dominant path of electron transfer in PS II is likely to be along the D1 polypeptide. However, in D1/D2 reaction centres without quinone present, it is likely that some of the charge separation may occur along the D2 polypeptide. Charge recombination of the radical pair on the D2 polypeptide to $P680^*$ may be the origin of one of the short fluorescence lifetimes, possibly the 1.5 ns component, which contributes to the D1/D2 fluorescence (see Analysis section). As yet there are no transient absorption data to indicate the branching ratio for

primary electron transfer in PS II reaction centres, so this model of parallel electron transfer has to be considered.

In the analysis of the fluorescence decays, the analysis procedure assumes the decay to be the sum of two or more exponentials. Although this may be the case, it is possible that the decay actually represents a continuous relaxation process where the equilibrium changes continuously over nanoseconds. In this case, treating the data as a sum of exponentials can only be a crude approximation to the real form of the fluorescence decay. The D1/D2 decays are best represented by the analysis program as the sum of four exponentials. The shortest lifetime of 0.1 ns is probably due to a combination of prompt fluorescence and scattered light and the 6.5 ns lifetime is assigned to chlorophyll unrelated to charge separation. The 37 ns lifetime is associated with charge separation and it is possible that the remaining lifetime, of approx. 1.5 ns, is also connected with this process. These two lifetimes may be due to two independent equilibria between $P680^*$ and different radical-pair states, possibly due to electron transfer along the D1 and D2 polypeptides, or to an initial radical-pair state that relaxes to another state of lower energy. The relaxations may be due to equilibration between the singlet and triplet states of the radical pair (see Fig. 1) or to nuclear relaxations. The former mechanism has been ruled out for bacterial reaction centres.

Substituting the appropriate values for the 1.5 ns component into Eqns. 1 and 2 allows $\Delta G(P680^+Ph^-P680^*)$ over this time to be estimated as -0.07 eV at 277 K. This free-energy difference could be due to an unrelaxed radical-pair state or to a radical pair on the D2 polypeptide. Temperature dependence of this free-energy difference indicates that the ΔG curve is approximately linear (Booth, P.J., unpublished data) with an entropy difference of approx. $-1.7 \cdot 10^{-4}$ eV \cdot K $^{-1}$ and a zero enthalpy change. However, a further study is required, using a shorter timescale, to determine these values accurately.

By analogy with the bacterial reaction centre, the 37 ns lifetime may correspond to a relaxed radical pair, while the 1.5 ns lifetime may correspond to an unrelaxed state.

Conclusion

The majority of the fluorescence from D1/D2 reaction centres is from 6.5 ns and 37 ns components. The yields of these decay components are $(40 \pm 5)\%$ and $(44 \pm 4)\%$, respectively. The 37 ns decay is assigned to an equilibrium between $P680^*$ and the primary radical pair, while the 6.5 ns component is due to contaminating chlorophyll which is uncoupled from the electron transfer. The yield of the charge-recombination component is a very sensitive measure of the integrity of the

D1/D2 complex. 94% of the chlorophyll present in the intact D1/D2 samples is associated with charge separation.

The free-energy change associated with electron transfer from P680* to the radical pair in PS II reaction centres is -0.11 eV at 277 K. From 77 K to 220 K this free-energy change is dominated by the entropy change, which is $3.8 \cdot 10^{-4}$ eV \cdot K $^{-1}$. Over this temperature range, the enthalpy contribution to the free-energy change is negligible, being only 6% of the total free-energy difference at 200 K. The temperature dependence of the free-energy difference between the excited special pair and the primary radical pair is very similar to that in purple bacteria, where the free-energy gap is dominated by the entropy change from 77 K to 200 K.

Acknowledgements

We would like to thank the European Commission, British Petroleum, SERC, AFRC and the Rowland Foundation for financial assistance. We also thank David Chapman and James Durrant for their kind advice and assistance and Jill Farmer for the preparation of the samples. Finally, we acknowledge Dr. R. Vogel and the EMBL for providing the analysis program SPLMOD.

References

- Nanba, O. and Satoh, K. (1987) *Proc. Natl. Acad. Sci. USA* 84, 109–112.
- Barber, J., Chapman, D.J. and Telfer, A. (1987) *FEBS Lett.* 220, 67–73.
- Crystall, B., Booth, P.J., Klug, D.R., Barber, J. and Porter, G. (1989) *FEBS Lett.* 249, 75–78.
- Danielius, R.V., Satoh, K., Van Kan, P.J.M., Plijter, J.J., Nuijs, A.M. and Van Gorkom, H.J. (1987) *FEBS Lett.* 213, 241–244.
- Takahashi, Y., Hansson, O., Mathis, P. and Satoh, K. (1988) *Biochim. Biophys. Acta* 893, 49–59.
- Seibert, M., Picorel, R., Rubin, A.B. and Connolly, J.S. (1988) *Plant Physiol.* 87, 303–306.
- Mimuro, M., Yamazaki, I., Itoh, S., Tamai, N. and Satoh, K. (1988) *Biochim. Biophys. Acta* 933, 478–486.
- Wasielewski, M.R., Douglas, G.J., Seibert, M. and Govindjee (1989) *Proc. Natl. Acad. Sci. USA* 86, 524–528.
- Durrant, J.R., Giorgi, L.B., Barber, J., Klug, D.R. and Porter, G. (1990) in *Current Research in Photosynthesis* (Baltseffsky, M., ed.), Vol. I, pp. 415–418, Kluwer, Dordrecht.
- Chapman, D.J., Gounaris, K. and Barber, J. (1989) *Photosynthetica* 23, 411–426.
- McTavish, H., Picorel, R. and Seibert, M. (1989) *Plant Physiol.* 89, 452–456.
- Giorgi, L.B., Crystall, B., Booth, P.J., Durrant, J.R., Barber, J., Klug, D.R. and Porter, G. (1989) in *Current Research in Photosynthesis* (Baltseffsky, M., ed.), Vol. II, pp. 519–522, Kluwer, Dordrecht.
- Chapman, D.J., Gounaris, K. and Barber, J. (1988) *Biochim. Biophys. Acta* 933, 423–431.
- O'Connor, D.V. and Phillips, D. (1984) *Time-Correlated Single Photon Counting*, Academic Press, London.
- Ide, J.P., Klug, D.R., Kühlbrandt, W., Giorgi, L.B. and Porter, G. (1987) *Biochim. Biophys. Acta* 893, 349–364.
- Marquardt, D.W. (1963) *J. Soc. Ind. Appl. Math.* 11, 431–441.
- Weber, G. and Teale, F.W.J. (1957) *Trans. Faraday Soc.* 53, 646–655.
- Woodbury, N.W.T. and Parson, W.W. (1984) *Biochim. Biophys. Acta* 767, 345–361.
- Owens, T.G., Webb, S.P., Alberte, R.S., Mets, L. and Fleming, G.R. (1988) *Biophys. J.* 53, 733–745.
- Kelly, J.M. and Porter, G. (1970) *Proc. R. Soc. A* 319, 319–329.
- Klimov, V.V., Klevanik, A.V., Shuvalov, V.A. and Krasnovsky, A.A. (1977) *FEBS Lett.* 82, 183–186.
- Ide, J.P. (1988) PhD Thesis, University of London.
- Butler, W.L. and Norris, K.H. (1963) *Biochim. Biophys. Acta* 66, 72–77.
- Ogrodnik, A., Volk, M., Letterer, R., Feick, R. and Michel-Beyerle, M.E. (1988) *Biochim. Biophys. Acta* 936, 361–371.
- Goldstein, R.A., Takiff, L. and Boxer, S.G. (1988) *Biochim. Biophys. Acta* 934, 253–263.
- Woodbury, N.W., Parson, W.W., Gunner, M.R., Prince, R.C. and Dutton, P.L. (1986) *Biochim. Biophys. Acta* 851, 6–22.
- Hörber, J.K.H., Göbel, W., Ogrodnik, A., Michel-Beyerle, M.E. and Cogdell, R.J. (1986) *FEBS Lett.* 198, 273–278.
- Hörber, J.K.H., Göbel, W., Ogrodnik, A., Michel-Beyerle, M.E. and Knapp, F.W. (1985) in *Antennas and Reaction Centres of Photosynthetic Bacteria* (Michel-Beyerle, M.E., ed.), pp. 292–297, Springer-Verlag, Berlin.
- Hörber, J.K.H., Göbel, W., Ogrodnik, A., Michel-Beyerle, M.E. and Cogdell, R.J. (1986) *FEBS Lett.* 198, 268–272.
- Michel-Beyerle, M.E., Plato, M., Deisenhofer, J., Michel, H., Bixon, M. and Jortner, J. (1988) *Biochim. Biophys. Acta* 932, 52–70.
- Kellogg, E.C., Kolaczowski, S., Wasielewski, M.R. and Tiede, D.M. (1989) *Photosynth. Res.* 22, 47–59.
- Aumeier, W., Eberl, U., Ogrodnik, A., Volk, M., Scheidel, G., Feick, R. and Michel-Beyerle, M.E. (1989) *Physiol. Plant.* 76, A32.
- Fleming, G.R., Martin, J.L. and Breton, J. (1988) *Nature* 333, 190–192.
- Goldstein, R.A. and Boxer, S.G. (1989) *Biochim. Biophys. Acta* 977, 78–86.
- Williams, J.C., Steiner, L.A., Feher, G. and Simon, M.I. (1984) *Proc. Natl. Acad. Sci. USA* 81, 7303–7307.
- Barber, J. (1987) *Trends Biochem. Sci.* 12, 321–326.
- Michel, H. and Deisenhofer, J. (1988) *Biochemistry* 27, 1–7.